On-line Parameter Identification and Self-Commissioning of Current Controller for Servo Motor Drives Considering Time Delay in Both Modeling and Control

Chih-Jung Hsu
Center for Power Electronics Technology
National Taipei University of Technology
Taipei, Taiwan

Yen-Shin Lai, Fellow IEEE
Center for Power Electronics Technology
National Taipei University of Technology
Taipei, Taiwan

***Abstract*—The main theme of this paper is to propose an on-line parameter identification and self-commissioning of current controller for servo motor drives as time delay is taken into consideration. The advantages of considering time delay include increase of current controller bandwidth and easy to achieve delay compensation. The electrical parameters and time delay required for self-commissioning of current controller are identified on-line through injecting signal and real-time Fast Fourier Transform (FFT) under standstill. The current controller gains are determined based upon the magnitude optimal method as the delay is considered while retaining the maximum phase margin.**

The experimental results will be shown, which are derived from DSP-controlled PMSM servo drives. With the proposed parameter identification method, in which time delay identification is included, the measured bandwidth of current loop is improved as compared with that without such consideration. These results confirm the effectiveness and claims of the proposed method.

Keywords—Servo Drives, PMSM, Current Control, Self-commissioning

I. INTRODUCTION

The cascade controllers of servo drives include current loop, speed loop and position loop, in general. Accordingly, the stability and bandwidth of current loop for servo drives are highly valued and are always regarded as performance indexes. In addition, to guarantee system stability and achieve fast dynamic performance, tuning of current controllers is demanded. Therefore, various parameter identification and automatic control gain tuning methods have drawn the interest of researchers [1]-[10].

High frequency signal injection method for inductance identification has been proposed in [1-4]. In [1], high frequency sinusoidal signal is injected as voltage reference in rotor reference frame and the induced current is extracted by the Discrete Fourier Transform (DFT) to calculate the inductance. In addition, the effect of inverter nonlinearities is considered. Similarly, the saturation and cross-saturation effects are taken into account during the inductance estimation in [2]. The method shown in [3] is proposed a stable current control, though motor parameters are unknown before parameter tuning is executed. Additionally, the on-line tuning methods are presented, such as parameter identification method based on Pulse-Width Modulation (PWM) predictive control [5], Model Reference Adaptive Scheme (MRAS) estimators [6], a q-axis inductance identification based upon the relationship between the mismatch of q-axis inductance and d-axis feedback current [7], and least square method is used for motor electrical parameters identification as shown in [8]-[9]. Moreover, the off-line tuning method [10] estimates the winding resistor and inductances at standstill by injecting two pulsating voltages. However, the amplitude or injecting time of the pulsating voltage should be well adjusted. The time delay contributed by the PWM control, filter and calculation, especially in the digital-controlled servo drives, has not yet been identified.

Based upon the survey of previous work as mentioned above, the gains of the current controller are usually designed by pole-zero cancellation [1], [7], and [9]-[10]. In reality, the voltage output is inevitably delayed in a full-digital current control system because of the PWM control, filter and calculation. The digital time delay will affect the system instability and current loop bandwidth [11]-[12]. Therefore, delay issue should be considered in the current controller design. To do this and/or compensate such delay to increase the bandwidth of current control loop, time delay should be clearly identified.

The main theme of this paper is to propose an on-line parameter identification and self-commissioning of current controller for servo motor drives as time delay is taken into consideration. The advantages of considering time delay include increase of current controller bandwidth and easy to achieve delay compensation. The electrical parameters and time delay required for self-commissioning of current controller are identified on-line through injecting signal and real-time Fast Fourier Transform (FFT) under standstill. The current controller gains are determined based upon the magnitude optimal method as the delay is considered while retaining the maximum phase margin.

The experimental results will be shown, which are derived from DSP-controlled PMSM servo drives. These results confirm the feasibility and claims of the proposed method.

978-1-5090-6684-1/18/$31.00 ©2018 IEEE

II. PROPOSED PARAMETER IDENTIFICATION METHOD

In Flux Oriented Control (FOC) of PMSM, the rotational transformations, decoupling, and the back EMF feed-forward compensation are applied. Therefore, the remaining plant can be considered as a time delay system with a current model including stator resistor and inductance which give the motor electrical time constant [13]. Furthermore, the time delay in the digital control systems usually is caused by sampling delay, T_{fb}, and the calculation delay, T_{proc}, and PWM switching active delay, T_{PWM}. In addition, the PWM switching active delay can be modeled by zero-order hold (ZOH). Thus, the overall time delay $T_{\Sigma I}$ can be obtained as shown in (1). Moreover, the plant transfer function, G_{CI}, is shown in (2). As shown in Fig. 1, the q-axis current loop is derived from PI controller, system delay $T_{\Sigma I}$, motor electrical model and feedback. K_{PI} and T_{NI} are PI controller's gain and time constant, respectively. Therefore, the proposed method of parameters identification can be developed based upon the transfer function using the injection chirp wave at standstill, and rebuilding the Bode plot through FFT.

$$T_{\Sigma I} = T_{fb} + T_{proc} + T_{PWM} \tag{1}$$

$$G_{CI}(s) = \frac{1}{R_s + sL_{qs}} e^{-sT_{\Sigma I}} \tag{2}$$

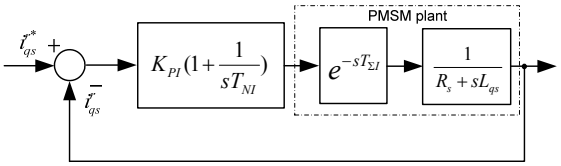

Fig. 1. The q-axis current control loop.

The current model can be rewritten as a first-order lag model, as shown in (3), where $K_a = 1/R_s$, and $t_e = L_{qs}/R_s$ is motor electrical time constant. In addition, based upon Bode plot of the first-order lag model, K_a and t_e can be founded by find out the DC gain and the frequency of -45 degrees, as shown in (4) and (5), respectively.

$$T_{RL}(s) = \frac{i_q^r(s)}{V_q^r(s)} = \frac{1}{R_s + sL_{qs}} = \frac{K_a}{1 + t_e s} \tag{3}$$

$$DC_{gain} = 20\log K_a \tag{4}$$

$$f_{-45^\circ} = \frac{1}{2\pi t_e} \tag{5}$$

Therefore, the motor electrical parameters can be identified by the Bode plot. Moreover, the Laplace transform of time delay function can be represented in (6), and the magnitude and phase response can be obtained by Euler's formula as shown in (7) and (8), respectively. Hence, it is noted that time delay affects in phase, but does not have effects on magnitude. In general, the time delay has more relevant influence in high frequency range. In short, according to these characteristics the current model can be identified as follows.

First, the DC gain and the frequency of -45 degrees can be founded at low frequency band, and then the electrical parameters can be identified.

Second, the phase response of time delay can be obtained through the Bode plot and the identified electrical parameters.

Finally, the time delay can be calculated by (8).

$$G_d(s) = e^{-sT_{\Sigma I}} \tag{6}$$

$$\left| e^{-sT_{\Sigma I}} \right|_{s=j\omega} = \left| \cos(\omega T_{\Sigma I}) + j\sin(\omega T_{\Sigma I}) \right| = 1 \tag{7}$$

$$\angle e^{-sT_{\Sigma I}} = \tan^{-1}\left(\frac{-\sin(\omega T_{\Sigma I})}{\cos(\omega T_{\Sigma I})} \right) = -\omega T_{\Sigma I} \tag{8}$$

The chirp function outputs a swept-frequency cosine signal with unity amplitude and continuous phase, so the signal can be used for deriving the frequency response of the tested system [14]. The corresponding time domain function for a sinusoidal linear chirp is given in (9), where f_0 is the starting frequency, and k is the rate of frequency change. In addition, for a Linear Time-Invariant (LTI) system, the Fourier transform of the output, $Y(e^{j\omega})$, is derived by multiplying the Fourier transform of the input, $X(e^{j\omega})$, and the Fourier transform of the LTI system, $H(e^{j\omega})$, as shown in (10). Furthermore, the Fourier transform of the LTI system can be obtained from $Y(e^{j\omega})$ divided by $X(e^{j\omega})$. Thus, the magnitude response and phase response of $H(e^{j\omega})$ are given in (11) and (12), respectively. Therefore, the Bode plot rebuilding method based upon this idea and FFT is adopted in this paper, and the method can be easily integrated into the DSP-based servo drives while not requiring the analyzer. Therefore, the electrical parameters including the time delay can be identified ***on-line*** using only DSP software.

$$x(t) = \sin\left[\Phi_0 + 2\pi\left(f_0 t + \frac{k}{2} t^2 \right) \right] \tag{9}$$

$$Y(e^{jw}) = X(e^{jw}) \cdot H(e^{jw}) \tag{10}$$

$$\left| H(e^{jw}) \right| = \frac{\left| Y(e^{jw}) \right|}{\left| X(e^{jw}) \right|} \tag{11}$$

$$\angle H(e^{jw}) = \angle Y(e^{jw}) - \angle X(e^{jw}) \tag{12}$$

The gains of current controllers considering the time delay can be determined once the current model is derived based upon *magnitude optimum method* [15-16]. The time constant of current controller, $T_{NI,}$ is set to motor electrical time constant to give the open loop transfer function as shown in (13). However, to further simplify the transfer function, two normalized coefficients are introduced. One is control gain related, γ, and the other is frequency related, Ω, as shown in (14) and (15), respectively. Hence, the open loop transfer function can be rewritten by substituting the normalized coefficients into (13) to give (16). Considering the time delay in the current model, the controller gain K_{PI} and time constant T_{NI} based upon the magnitude optimum method [13], [15] can be determined as shown in (17) and (18) for the given phase margin = 61 degrees and γ = 0.5. These results will provide an *on-line self-commissioning* of current controller *with considering the time delay.*

$$F_{OI}(s)=\frac{K_{PI}}{L_{qs}}\frac{e^{-sT_{\Sigma I}}}{s} \tag{13}$$

$$\gamma=\frac{K_{PI}T_{\Sigma I}}{L_{qs}} \tag{14}$$

$$\Omega=\omega T_{\Sigma I} \tag{15}$$

$$F_{OI}(j\Omega)=\gamma\frac{e^{-j\Omega}}{j\Omega} \tag{16}$$

$$K_{PI}=0.5\frac{L_{qs}}{T_{\Sigma I}} \tag{17}$$

$$T_{NI}=t_e=\frac{L_{qs}}{R_s} \tag{18}$$

The block diagram of proposed on-line parameters identification method is shown in Fig. 2. The q-axis or d-axis parameters identification is selected through the terminal 1 or 2 correspondingly. In addition, the current control after self-commissioning can work by selected through the terminal 3. For example, for q-axis parameters identification, a sinusoidal linear chirp as given in (9) is injected into the q-axis voltage command and the d-axis voltage command is zero, Then, the q-axis parameters include resistance, inductance and time delay can be identified on-line through the Bode plot rebuilding method as mentioned above using DSP software. After that, the current controller gains can be automatically tuned with considering the time delay to achieve self-commissioning of current loop control.

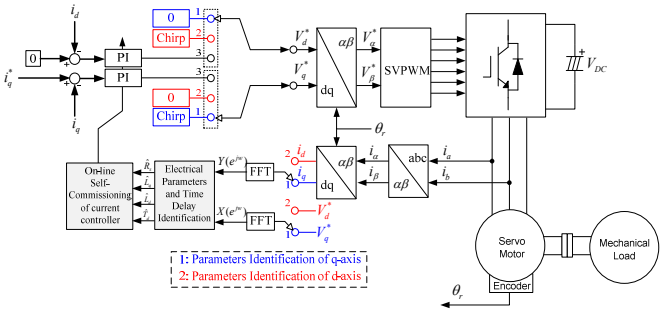

Fig. 2. The system block diagram of proposed on-line parameter identification and self-commissioning of current control.

Fig. 3 shows the flow chart of proposed parameter identification and self-commissioning of current control technique based upon the Bode plot rebuilding method. The flow chart shown in Fig. 4 is Bode plot rebuilding method based. In Fig. 4, "*x*" could be q-axis or d-axis component, which is selected through the terminal 1 or 2. For example, for q-axis transfer function, a sinusoidal linear chirp as given in (9) is injected into the q-axis voltage command. Then, the Bode plot can be obtained from (11) and (12).

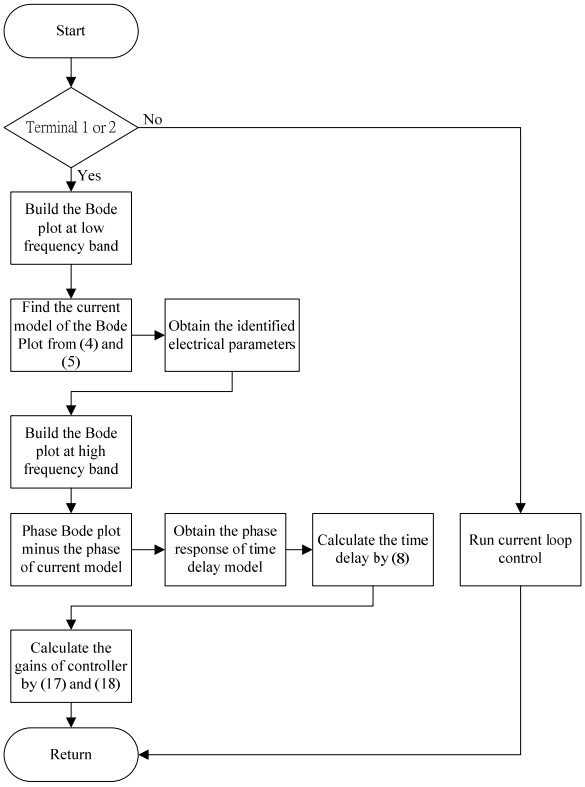

Fig. 3. Flow chart, proposed identified and self-commission method.

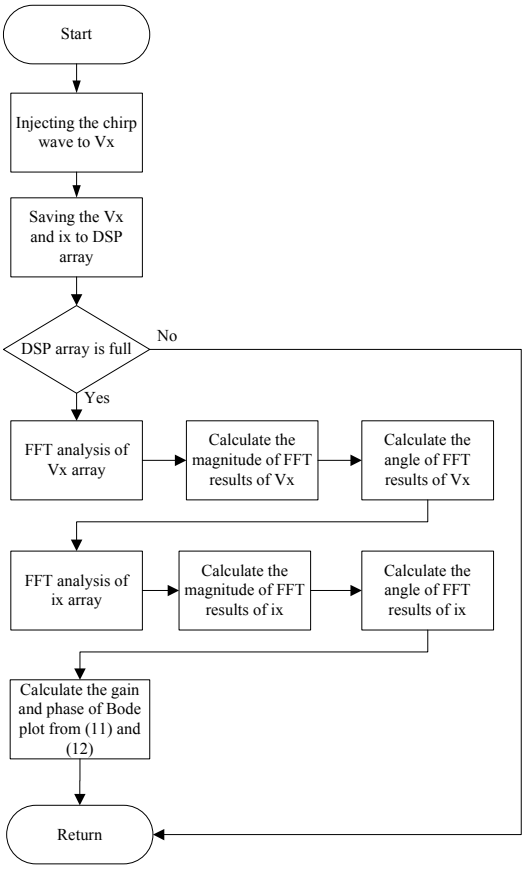

Fig. 4. Flow chart, proposed Bode plot rebuiling method.

III. Simulation Results

Theoretical derivation and analysis are provided as previously mentioned. To verify the validation of the proposed method, simulation is carried out by Matlab/Simulink as shown in Fig. 5. The parameters of simulation are listed in Table I, and the time delay parameter of simulation is designed to be 75 us.

The simulation results are shown in Fig. 6 and Fig. 7. The time response of current model with time delay in two different frequency bands is shown in Fig. 6. Fig. 7(a) shows the Bode plot of the current model of q-axis with delay model. As shown in Fig. 7(a), the *red line* denotes the current model which is created by the searching results of DC gain and the frequency of -45 degreed, and the magnitude of the Bode plot is similar to that of the theoretical model. In addition, the phase of the Bode plot shows the phase delay effect of the time delay. Moreover, the *blue line* indicates the simulation result derived using the proposed method, which considers time delay as shown in Fig. 7(b). The identified time delay is about 74.7 μs, which is very close to the designed parameter.

TABLE I
PARAMETERS OF THE SIMULATION

Symbol	Meaning	Value
R_s	Stator resistance	1.875 Ω
L_{qs}	Stator inductance	7.65 mH
$T_{\Sigma I}$	System time delay	75 us

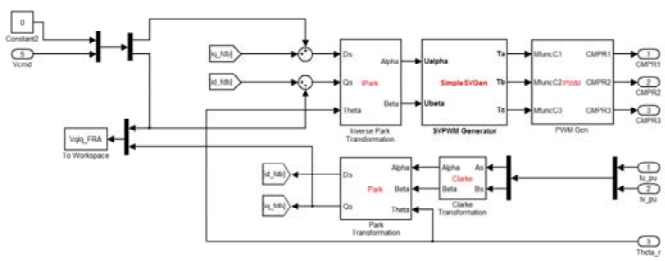

Fig. 5. Simulation block diagram by Matlab/Simulink .

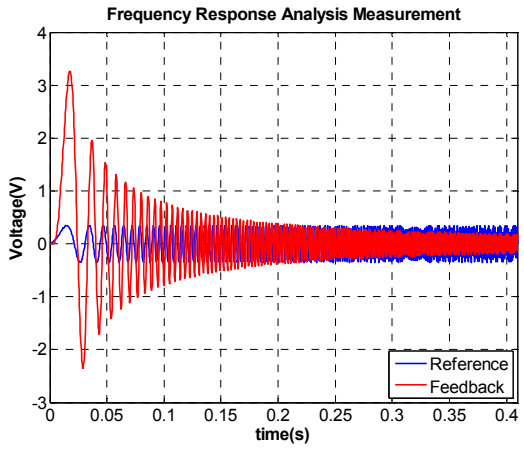

(a)

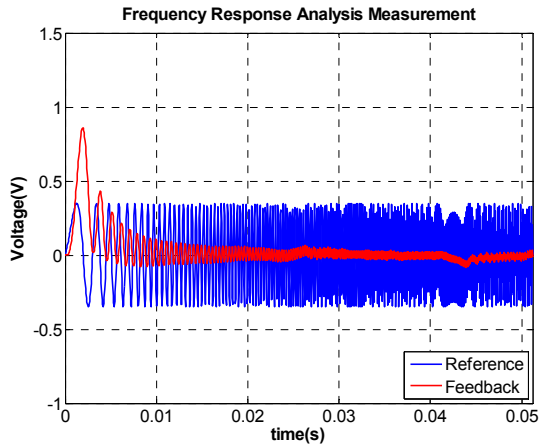

(b)

Fig. 6. Simulation results, the time response of current model with time delay, (a) low frequency band, (b) high frequency band.

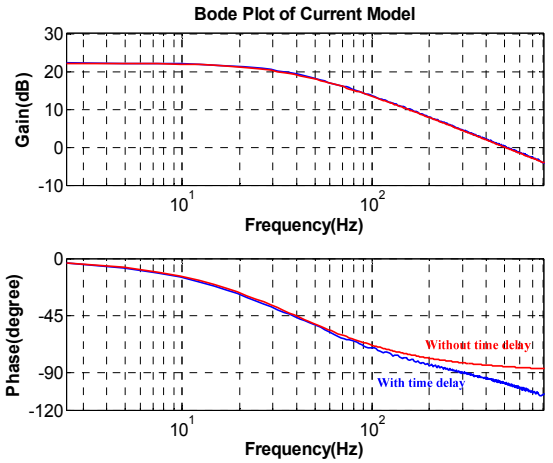

(a) current model

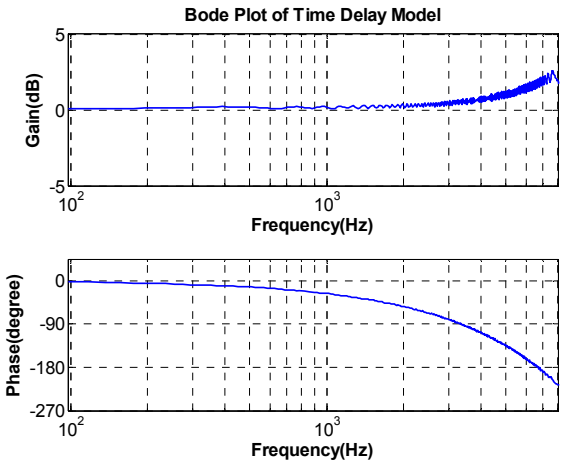

(b) time delay model

Fig. 7. Simulation results, identified model with/without considering time delay using proposed identified method.

IV. Experimental Results

The presented method is realized by a DSP-based controller in software with TI DSP TMS320F28335. A 400 W PMSM servo motor is used and the photo of the test set-up is shown in Fig. 8. Besides, the Gain and Phase Analyzer (PSM1735) is used for verifying the proposed method and comparing with the identification results of DSP-based servo drive. Moreover, the load motor is used to lock the rotor of the servo motor when injecting the chirp wave, and the specifications of experimental system are summarized in Table II. In this paper, the length of FFT array is 1024, the PWM frequency is 10 kHz.

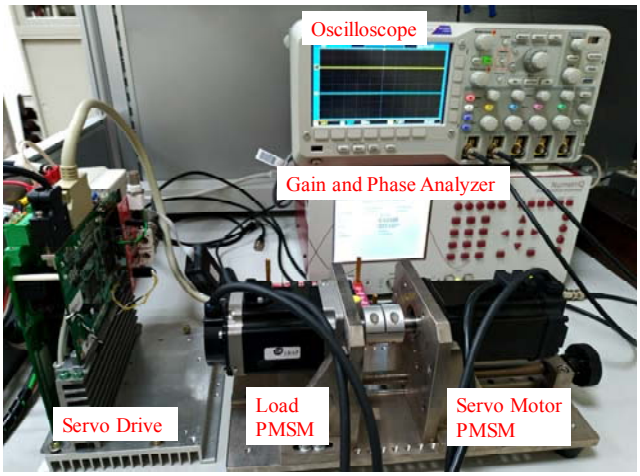

Fig. 8. Experimental system.

TABLE II
PARAMETERS OF THE SERVO DRIVES SYSTEM AND CONTROLLER

Symbol	Meaning	Value
P_R	Rate Power (W)	400
T_R	Rate Torque (N-m)	1.27
N_R	Rate Speed (rpm)	3000
I_R	Rate Current (A)	2.45
K_T	Torque constant (N-m/A)	0.52
t_e	Electical time constant (ms)	4.08
Pole	Number of pole pairs	8
ADC	The resolution bit of ADC	12
f_{sys}	System clock (MHz)	150
f_{sw}	PWM frequency (kHz)	10
f_{si}	Current sampling frequency (kHz)	20

The experimental results with Gain and Phase Analyzer(PSM1735) are shown in Fig. 9 to Fig. 10. Fig. 9 shows the process of system analysis at two different frequency bands with PSM1735. And the sweep time of two frequency zone is 7.8s and 6.9s, respectively. Fig. 10 shows the Bode plot of the plant, G_{CI}, shown in (2). As shown in Fig. 10, the *red line* denotes current model which is created by searching of DC gain and the frequency of -45 degree, and the *blue line* indicates the analysis result from PSM1735. Additionally, the identified time delay model is shown in Fig. 10(b), and the identified time delay is about 71.1us.

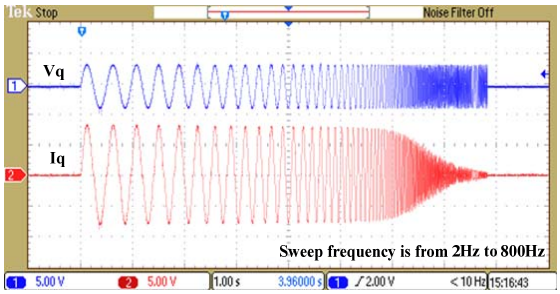

(a)

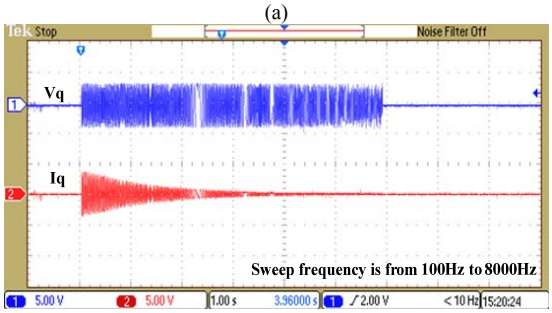

(b)

Fig. 9. Experimental results, the time response using PSM1735, (a) low frequency band, (b) high frequency band.

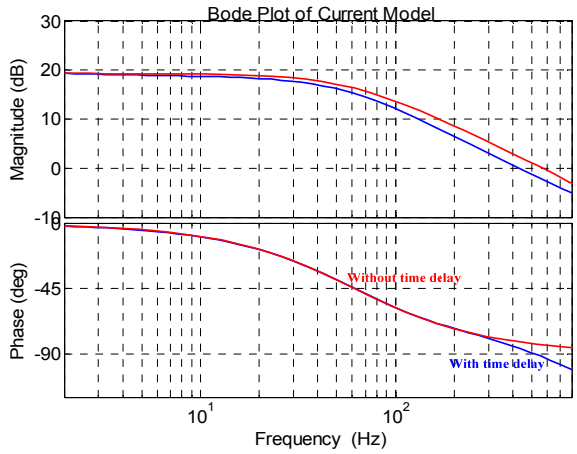

(a) current model

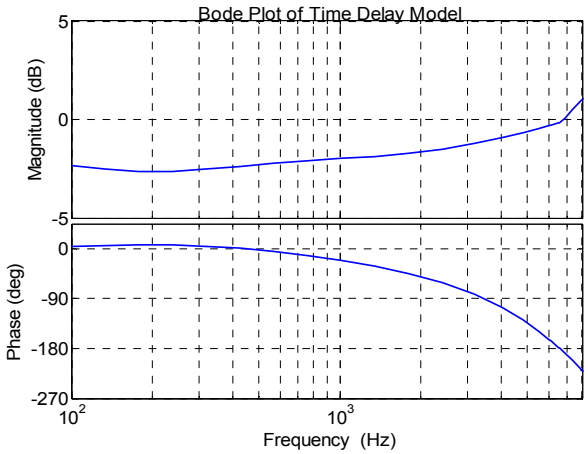

(b) time delay model

Fig. 10. Experimental results using PSM1735, identified model with/without considering time delay using proposed identified method.

Similarly, the experimental results of DSP-based are shown in Fig. 11 to Fig. 12. The process of system analysis at two different frequency bands is shown in Fig. 11, and because of the linear of chirp frequency, the response is different to Fig. 9. Therefore, the sweep time of two frequency zone is 0.4s and 51.2ms, respectively. Thus, the exciting time is quite short, so the proposed method can effectively shorten the identified time. As shown in Fig. 12(a), the *red line* denotes current model which is created by searching of DC gain and the frequency of -45 degrees, which means no time delay is considered. And the *blue line* indicates the test results derived using the proposed method which considers time delay as shown in Fig. 12(b), and the identified time delay is calculated about 70.0us. As the results, Fig. 12(b) is similar to Fig. 10(b) and thereby confirming the proposed method.

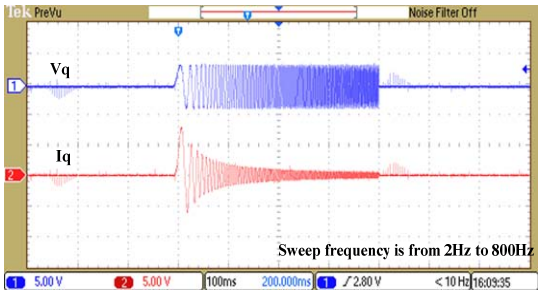

(a)

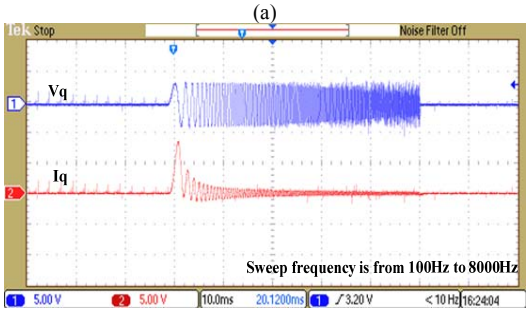

(b)

Fig. 11. Experimental results, the time response of DSP-based, (a) low frequency band, (b) high frequency band.

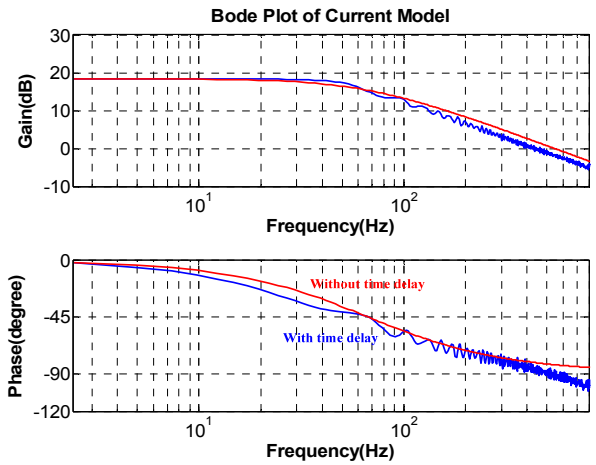

(a) current model

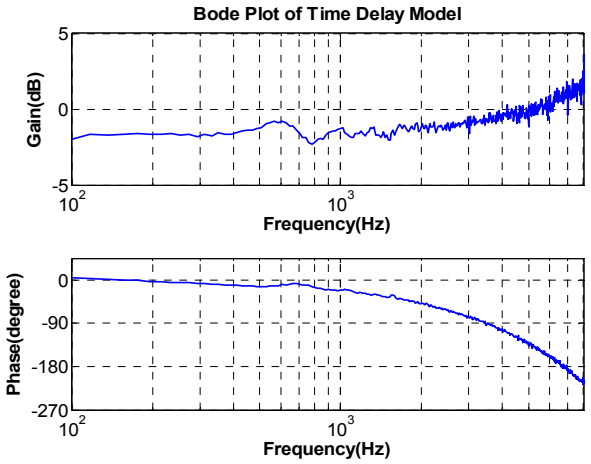

(b) time delay model

Fig. 12. Experimental results of DSP-based, identified model with/without considering time delay using proposed identified method.

Based upon the identified current model with/without considering the time delay, the controller gains are on-line generated using (17) and (18). After that, the Bode of the current loop is measured using Frequency Response Analyzer, PSM1735. For further confirmation, the measured Bode plot of the current closed-loop is given in Fig. 13, where the *red line* indicates the calculated gain *without* considering the time delay, and the *blue line* denotes the gain calculated with considering the time delay. Obviously, the -3dB bandwidth is improved from 1650 Hz to 1910 Hz as time delay is considered based upon the proposed on-line parameter identification method.

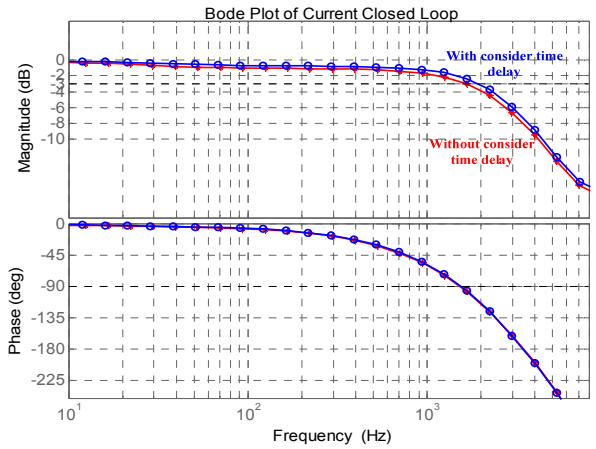

(a)

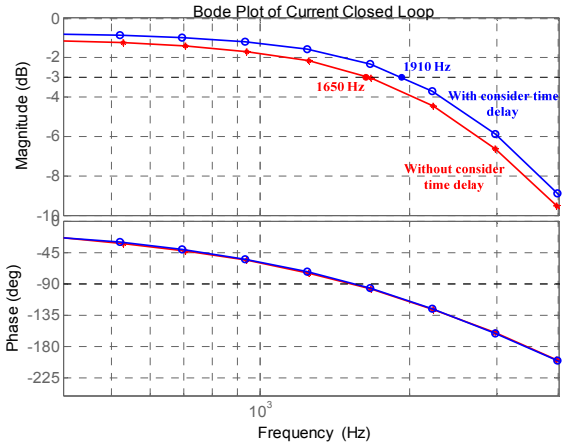

(b)

Fig. 13. Measured result using PSM1735, Bode Plot of closed current loop designed with/without considering time delay.

V. Conclusions

An on-line parameter identification and self-commissioning of current controller for servo motor drives as time delay is considered is presented. The advantages of considering time delay include increase of current controller bandwidth and easy to achieve delay compensation. The electrical parameters and time delay required for self-commissioning of current controller are identified on-line through injecting signal and real-time Fast Fourier Transform (FFT) under standstill. The current controller gains are determined based upon the magnitude optimal method as the delay is considered while retaining the maximum phase margin. Experimental results show the parameters as well as the time delay contributed by calculation, feedback, and PWM generation, etc. can be identified on-line. With the proposed parameter identification method, in which time delay identification is included, the measured bandwidth of current loop is improved as compared with that without such consideration. These results confirm the effectiveness and claims of the proposed method.

References

[1] G. Wang, L. Qu, H. Zhan, J. Xu, L. Ding, G. Zhang, and D. Xu, "Self-commissioning of permanent magnet synchronous machine drives at standstill considering inverter nonlinearities," IEEE Trans. on Power Electron., vol. 29, no. 12, pp. 6615–6627, Dec. 2014.

[2] G. Feng, C. Lai, and N. Kar, "A novel current injection-based online parameter estimation method for PMSMs considering magnetic saturation," IEEE Trans. on Magnetics, vol. 52, no. 7, pp. 1-4, Jul. 2016.

[3] N. Nomura and S. Higuchi, "Auto-tuning method of inductances for permanent magnet synchronous motors," International Power Electronics Conference (IPEC-Hiroshima 2014 – ECCE-ASIA), 2014.

[4] Cristian Lascu and Gheorghe-Daniel Andreescu, "Self-commissioning of electrical parameters for PMSM in sensorless drives," Electrical Machines & Power Electronics (ACEMP) 2015 Intl Conference on Optimization of Electrical & Electronic Equipment (OPTIM) & 2015 Intl Symposium on Advanced Electromechanical Motion Systems (ELECTROMOTION) 2015 Intl Aegean Conference on, pp. 605-610, 2015.

[5] J. Long, M. Yang, X. Y. Lang, X. Lv, X. S. Liu, and D. G. Xu, "Advanced online parameter identification-based PWM predictive control for AC servo systems," IECON 2016 - 42nd Annual Conference of the IEEE, pp. 2672-2677, 2016.

[6] Y. Zhang, Z. Yin, X. Sun, and Y. Zhong, "On-line identification methods of parameters for permanent magnet synchronous motors based on cascade MRAS," in Proc. 9th Int. Conf. Power Electron. ECCE Asia, Seoul, Korea, pp. 345–353, Jun. 2015.

[7] X. Ji, T. Noguchi, "Online q-axis inductance and resistance identification of IPM synchronous motor based on relationship between its parameter mismatch and current," Electrical Machines and Systems (ICEMS) 2015 18th International Conference on, pp. 648-653, 2015.

[8] S. Morimoto, M. Sanada, and Y. Takeda, "Mechanical sensorless drives of IPMSM with online parameter identification," IEEE Transactions on Industry Applications, vol. 42, no. 5, pp. 1241–1248, 2006.

[9] D. Tadokoro, S. Morimoto, Y. Inoue, and M. Sanada, "Method for auto-tuning of current and speed controller in IPMSM drive system based on parameter identification," International Power Electronics Conference (IPEC-Hiroshima 2014 - ECCE-ASIA), pp. 390-394, 2014.

[10] S. M. Yang and K. W. Lin, "Automatic control loop tuning for permanent magnet ac servo motor drives," IEEE Transactions on Industrial Electronics, vol. 63, no. 3, pp. 1499-1506, Mar. 2016.

[11] G. Z. Zhang, F. Zhao, Y. X. Wang, X. Wen, and W. Cong, "Analysis and optimization of current regulator time delay in Permanent Magnet Synchronous Motor drive system," IEEE International Conference on Electrical Machines and Systems (ICEMS), 2013.

[12] B. H. Bae and S. K. Sul, "A compensation method for time delay of full-digital synchronous frame current regulator of PWM AC drives," IEEE Trans. on Industry Applications, vol. 39, no. 3, pp. 802–810, May/Jun. 2003.

[13] J. Böcker, S. Beineke, and A. Bähr, "On the control bandwidth of servo drives," EPE 2009, Barcelona, Spain.

[14] G. Franklin, J. Powell, and A. Emami-Naeini, "Feedback control of dynamic systems," Upper Saddle River, NJ: Prentice Hall, 2002, pp. 366-387.

[15] M. H. Ho and Y. S. Lai, "Controller design of servo drives for bandwidth improvement," IEEE 3rd International Future Energy Electronics Conference and ECCE Asia (IFEEC 2017 - ECCE Asia), 2017.

[16] M. H. Ho and Y. S. Lai, "Self-commissioning technique for high bandwidth servo motor drives," in proc. IEEE Energy Conversion Congress and Expo. (ECCE), 2017.